Journal of Geodynamics 97 (2016) 22–30

Contents lists available at ScienceDirect

Journal of Geodynamics

journal homepage: http://www.elsevier.com/locate/jog

On a spectral method for forward gravity field modelling

B.C. Root[a,*], P. Novák[b], D. Dirkx[a,d], M. Kaban[c,f], W. van der Wal[a], L.L.A. Vermeersen[a,e]

[a] Delft University of Technology, Kluyverweg 1, 2629 HS Delft, The Netherlands
[b] University of West Bohemia, Univerzitni 8, 306 14 Pilsen, Czech Republic
[c] Helmholtz Center Potsdam, GFZ German Research Center for Geosciences, Potsdam, Germany
[d] Joint Institute for VLBI ERIC, PO Box 2, 7990 AA Dwingeloo, The Netherlands
[e] NIOZ, Korringweg 7, 4401 NT Yerseke, The Netherlands
[f] Schmidt Institute of Physics of the Earth, RAS, Moscow, Russia

ARTICLE INFO

Article history:
Received 11 December 2015
Received in revised form 18 February 2016
Accepted 20 February 2016
Available online 23 February 2016

Keywords:
Forward gravitational field modelling
Spherical harmonic representation
Global density models

ABSTRACT

This article reviews a spectral forward gravity field modelling method that was initially designed for topographic/isostatic mass reduction of gravity data. The method transforms 3D spherical density models into gravitational potential fields using a spherical harmonic representation. The binomial series approximation in the approach, which is crucial for its computational efficiency, is examined and an error analysis is performed. It is shown that, this method cannot be used for density layers in crustal and upper mantle regions, because it results in large errors in the modelled potential field. Here, a correction is proposed to mitigate this erroneous behaviour. The improved method is benchmarked with a tesseroid gravity field modelling method and is shown to be accurate within ± 4 mGal for a layer representing the Moho density interface, which is below other errors in gravity field studies. After the proposed adjustment the method can be used for the global gravity modelling of the complete Earth's density structure.

1. Introduction

Interpreting gravitational data in terms of internal mass density distributions requires gravitational reduction that can be computed by forward modelling techniques. The gravitational field of any 3D object can be computed by integrating the gravitational effects of its mass density distribution. One technique for evaluating this integral is based on spherical harmonic expansion of the Newtonian kernel. This technique was applied to forward modelling of the topographic potential and its gradients (Lachapelle, 1976; Rapp, 1982; Rummel et al., 1988; Pavlis and Rapp, 1990) and modified for computing gravitational gradients generated by topography and atmosphere at satellite altitudes (Novák and Grafarend, 2006). The advantage of this technique is that it takes into account the curvature of the Earth.

There are two approaches to solve the spherical harmonic-based volume integral (Pavlis and Rapp, 1990): the rigorous formulation and the binomial series expansion method. The rigorous spectral method (RSM) introduced by Lachapelle (1976) is computational expensive (Pavlis and Rapp, 1990). The second approach, by Rummel et al. (1988), uses a binomial series expansion to approximate the volume. We call it the fast spectral method (FSM) in this study, because it is computationally more efficient than the rigorous spectral method. The number of computationally expensive global spherical harmonic analyses (GSHA) (Sneeuw, 1994) is drastically reduced by introducing the binomial series approximation. The FSM approach provides a means to use higher resolution density models than the RSM.

The FSM forward modelling is used in several previous studies (Rummel et al., 1988; Novák and Grafarend, 2006; Martinec, 1991; Root et al., 2015). Despite its computational speed, the FSM has limitations that should be known to users. The FSM forward modelling is used to compute the potential field of a topographic/isostatic mass layer in most studies, but for density layers in the lower crust and upper mantle the FSM gives erroneous results as will be shown in Section 4. This erroneous signal results in incorrect mantle density heterogeneities, when the FSM is used in a gravity inversion study. The improvement which is introduced here extends the applicability of the FSM to the general case of forward gravitational modelling of mass density distributions for an entire planet.

Section 2 provides a review of the analytical representation of the FSM. This is followed by a characterisation of the error introduced by the binomial series approximation. In Section 4, a mitigation strategy is introduced. Finally, a benchmark of the FSM with tesseroid software is shown in Section 5.

* Corresponding author.
E-mail address: b.c.root@tudelft.nl (B.C. Root).

http://dx.doi.org/10.1016/j.jog.2016.02.008
0264-3707/

2. Review of the fast spectral forward modelling method

The analytical representation of the RSM and FSM starts similarly (Pavlis and Rapp, 1990). In the following, we derive a formula for the gravitational potential which is the conventional representation of a (conservative and irrotational) gravitational field. From Newton's law of universal gravitation and the superposition principle, the gravitational potential V outside the body Σ at location, P, can be computed (e.g. Rummel et al. (1988)):

$$V(P) = G \int\int\int_{\Sigma} \frac{\rho(Q)}{\ell(P,Q)} \, \mathrm{d}\Sigma(Q). \tag{1}$$

where G is the universal gravitational constant, ρ is the mass density distribution within the body Σ and $\ell(P, Q)$ is the Euclidian distance between the computation point $P(r, \Omega)$ and the infinitesimal volume element $\mathrm{d}\Sigma(Q)$ at location $Q(r', \Omega')$. Eq. (1) can be rewritten by using (geocentric) spherical coordinates:

$$\mathrm{d}\Sigma = r^2 \mathrm{d}r \mathrm{d}\Omega. \tag{2}$$

Here, r is the radial coordinate and $\mathrm{d}\Omega = \sin(\theta)\mathrm{d}\theta \mathrm{d}\lambda$ is a surface element at a unit sphere, where ϕ and λ stand for a pair of geocentric angular coordinates and represents a geocentric direction. Eq. (1) then becomes

$$V(r,\Omega) = G \int_{\Xi} \int_{r'=r_{\mathrm{lower}}(\Omega')}^{r_{\mathrm{upper}}(\Omega')} \rho(r',\Omega') \;\; \mathcal{L}^{-1}(r,\Omega,r',\Omega') \;\; r'^2 \;\; \mathrm{d}r' \;\; \mathrm{d}\Omega'. \tag{3}$$

The kernel function $\mathcal{L}^{-1}(r,\Omega,r',\Omega') = \frac{1}{\ell(P,Q)}$ and the radial coordinate is given by r'. The radial limits of this integral represent the upper and lower boundaries of the mass density layer. The spherical harmonic representation for the inverse distance kernel is Heiskanen and Moritz (1984, p. 33):

$$\mathcal{L}^{-1}(r,\Omega,r',\Omega') = \frac{1}{r}\sum_{n,m}^{\infty}\left(\frac{r'}{r}\right)^{n} \frac{1}{2n+1} \;\; Y_{nm}(\Omega) \;\; Y^{*}_{nm}(\Omega'). \tag{4}$$

In this equation the abbreviated notation $\sum_{n,m}^{\infty} = \sum_{n=0}^{\infty}\sum_{m=-n}^{n}$ is used. Eq. (4) can be substituted in Eq. (3):

$$V(r,\Omega) = G\sum_{n,m}^{\infty}\left(\frac{1}{r}\right)^{n+1}\frac{1}{2n+1} \;\; Y_{nm}(\Omega) \;\; \int_{\Xi} \rho(\Omega') \;\; Y^{*}_{nm}(\Omega')$$
$$\mathrm{d}\Omega' \int_{r_{\mathrm{lower}}(\Omega')}^{r_{\mathrm{upper}}(\Omega')} r'^{n+2}\mathrm{d}r'. \tag{5}$$

where it is assumed that the density distribution within the layer does not depend on the radial position. Appendix A discusses an approach for a radially varying density distribution in the mass layer. For both cases, the radial integral in Eq. (5) must be evaluated. The radial limits of this integral can be defined as follows:

$$r_{\mathrm{upper}}(\Omega') = R + U(\Omega') \tag{6a}$$

$$r_{\mathrm{lower}}(\Omega') = R + L(\Omega'). \tag{6b}$$

$U(\Omega')$ and $L(\Omega')$ are upper and lower deviations from the circumscribing sphere (R) of the volumetric mass layer that is forward modelled (see Fig. 1). This means that $R \geq R + U \geq R + L$, or in other words $0 \geq U \geq L$. Integrating the radial integral of Eq. (5) then yields

$$\int_{r_{\mathrm{lower}}(\Omega')}^{r_{\mathrm{upper}}(\Omega')} r'^{n+2} \;\; \mathrm{d}r' = \frac{1}{n+3} \;\; \left\{ \underbrace{[R+U(\Omega')]^{n+3}}_{\text{1st part}} - \underbrace{[R+L(\Omega')]^{n+3}}_{\text{2nd part}} \right\}. \tag{7}$$

From this point the RSM and the FSM differ. In the RSM a global spherical harmonic analysis (GSHA) is performed on Eq. (7) to determine the spherical harmonic coefficients of the potential field (Lachapelle, 1976). However, this is computationally expensive, because for every degree (n) an individual GSHA must be performed. Especially, when the spherical harmonic degree is large the time to compute the potential field is unpractical. The FSM was developed to tackle this problem.

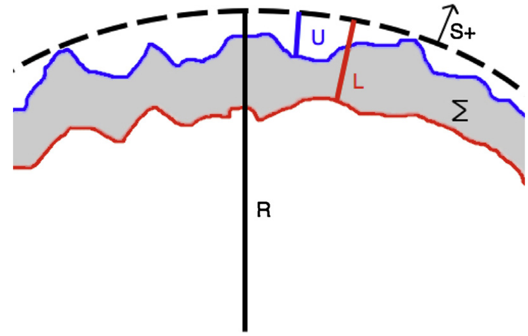

Fig. 1. Sketch of an arbitrary mass body. The distance (S) from the reference sphere R is defined positive upwards, resulting in $0 \geq U \geq L$.

In the FSM, the first and second part in Eq. (7) can be evaluated by a binomial series expansion (Abramowitz and Stegun, 1972). Writing $n + 3 = \nu$ and replacing U and L by their normalised values $\tilde{U} = \frac{U}{R}$ and $\tilde{L} = \frac{L}{R}$, we get

$$(R+U)^{\nu} - (R+L)^{\nu} = R^{\nu}\sum_{k=0}^{\nu} \;\; \binom{\nu}{k} \;\; \left[\tilde{U}^{k} - \tilde{L}^{k}\right]. \tag{8}$$

The series summation contains a finite number of terms, as ν is a positive integer (Abramowitz and Stegun, 1972). To reduce the computational load, in practical applications (Rummel et al., 1988) this series is truncated at a value α, where $\alpha < \nu$, resulting in

$$(R+U)^{\nu} - (R+L)^{\nu} = R^{\nu}\sum_{k=0}^{\alpha}\binom{\nu}{k} \;\; \left[\tilde{U}^{k} - \tilde{L}^{k} \;\; \right] + \epsilon_{\alpha}. \tag{9}$$

Here, ϵ_{α} is the error made by the truncation of the binomial series. An error analysis of this assumption follows in Section 3.1, but for now we will choose $\alpha = 3$ (Rummel et al., 1988). By neglecting the higher-order terms, the radial integral from Eq. (7) becomes

$$\int_{r_{\mathrm{lower}}(\Omega')}^{r_{\mathrm{upper}}(\Omega')} r'^{n+2}\mathrm{d}r' \approx R^{n+3}\left[\frac{U(\Omega') - L(\Omega')}{R}\right.$$
$$\left. +(n+2)\frac{U^2(\Omega') - L^2(\Omega')}{2R^2} + (n+2)(n+1)\frac{U^3(\Omega') - L^3(\Omega')}{6R^3}\right]. \tag{10}$$

Following Novák and Grafarend (2006), we will use a short-hand notation, $F(\Omega')$, to denote everything between the square brackets of Eq. (10):

$$\int_{r_{\mathrm{lower}}(\Omega')}^{r_{\mathrm{upper}}(\Omega')} r'^{n+2} \;\; \mathrm{d}r' \approx R^{n+3}F(\Omega'). \tag{11}$$

Substituting Eq. (11) in Eq. (5) gives:

$$V(r,\Omega) = GR^2\sum_{n,m}^{\infty}\left(\frac{R}{r}\right)^{n+1}\frac{1}{2n+1} \;\; Y_{nm}(\Omega)\int_{\Xi} \rho(\Omega') \;\; F(\Omega')$$
$$Y^{*}_{nm}(\Omega') \;\; \mathrm{d}\Omega'. \tag{12}$$